

# Effect of a microstructure on the formation of self-assembled laser cavities in polycrystalline ZnO

H. C. Ong<sup>a)</sup>

*Department of Electronic Engineering, City University of Hong Kong, Hong Kong*

J. Y. Dai

*Institute of Metal Research, Chinese Academy of Sciences, People's Republic of China*

A. S. K. Li

*Physics Department, Chinese University of Hong Kong, Shatin, Hong Kong*

G. T. Du

*State Key Laboratory on Integrated Optoelectronics, Jilin University, People's Republic of China*

R. P. H. Chang and S. T. Ho

*Department of Electrical and Computer Engineering, Northwestern University, Illinois 60208*

(Received 7 July 2000; accepted for publication 2 April 2001)

The optical properties of polycrystalline ZnO have been studied to elucidate the occurrence of random laser action. The spatially-resolved refractive index has been mapped out by using the scanning electron energy loss spectroscopy across the grain boundary. It is observed that the refractive index decreases gradually when the probe beam is approaching to the grain boundary. A thin reflective layer of  $\sim 10$  nm is found to form in the vicinity of the grain boundary, which assists the optical scattering. The photon scattering factor of the reflective layer has been determined and is shown to correlate well with the results of the coherent backscattering method. Together with the cathodoluminescence studies, it is suggested that the overall structure, which includes the grain and grain boundary, determines the laser action in ZnO. © 2001 American Institute of Physics. [DOI: 10.1063/1.1374452]

Recently, there has been a great interest in studying the ZnO thin films for the applications in the short wavelength optoelectronic devices. In addition to its low lasing threshold and high optical gain,<sup>1,2</sup> ZnO is found to possess an ability of self-assembling laser cavities without any artificial implementation. The strong optical scattering occurred in the disordered ZnO can paradoxically assist the formation of random laser cavities.<sup>3,4</sup> We have used the electron energy loss spectroscopy (EELS) to study the microstructure of the ZnO thin films and have found the refractive index difference between the grain and grain boundary is the key factor in causing the light scattering.<sup>5</sup> However, the exact scenario behind the laser action of ZnO remains unresolved. In this letter, we have combined the results of spatially resolved EELS, coherent backscattering (CBS) method, and cathodoluminescence (CL) to understand the lasing mechanism of ZnO. It is observed that a reflective layer, with a width of 9–12 nm, is formed in the vicinity of the grain boundary. We have mapped out the overall profile of the reflective layer and link its influence to the degree of light scattering acquired from the CBS. Combining with the CL studies, we propose that the grain and grain boundary together play an important role in determining the laser action of polycrystalline ZnO.

ZnO thin films are deposited on amorphous fused quartz by pulsed laser deposition at the growth temperature of

550 °C and 700 °C monitored by an optical pyrometer.<sup>3,5</sup> The thickness of the films is measured to be  $\sim 4000$  Å by using a stylus profilometer. Spatially resolved EELS has been carried out using a Gatan 666 PEELS in a Hitachi HF-2000 field emission gun—transmission electron microscope (TEM) at 200 keV. An energy resolution of 0.1 eV has been determined by measuring the full width at half maximum (FWHM) of the zero loss peak. The current setup is capable of producing a 2 Å diameter beam with a spatial resolution higher than 1.7 nm.<sup>6</sup> The acquisition and conversion of the low loss spectra to the optical functions have been given previously.<sup>7,8</sup> These include the single-scattering deconvolution of removing the zero loss peak using Lorentzian peak fit, convergence and angular correction, and Kramers–Kronig analysis.<sup>5,7,8</sup> The degree of light scattering of the samples is estimated by using the CBS method. A frequency-doubled output ( $\lambda' = 410$  nm) of a Ti:Sapphire laser (150 kHz repetition rate, 2 ns pulsed width) is used as the probed light to avoid absorption. The scattering mean free path  $l$  is then determined by evaluating the angular width of the backscattering cone.<sup>3,4</sup> CL studies have been carried out in a scanning electron microscope using an Oxford Instruments MonoCL system.<sup>9</sup> An accelerating voltage of 6 kV and beam current of 2.33 nA, with an electron penetration depth of  $\sim 3100$  Å, are used for maximizing the light emissions evolved from the film bulk region. The excitation is kept at low power to avoid any physical damage in the films. All the measurements are carried out at room temperature.

<sup>a)</sup>Author to whom correspondence should be addressed; Electronic mail: ehcong@cityu.edu.hk

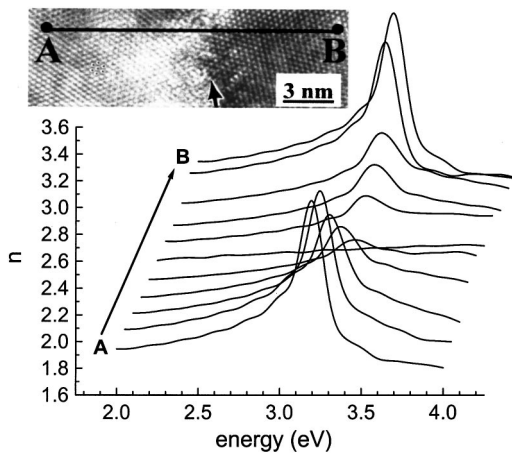


FIG. 1. The spatially resolved refractive index obtained from the conversion of the EELS data scanned across the grain boundary (from point A to B as shown in the inset) of the film grown at 700 °C. The inset shows the grain boundary structure. The arrow indicates the grain boundary.

The films grown at low and high substrate temperature are found to exhibit different structural properties. Cross section TEM shows two films have a columnar structure with the  $c$  axis preferentially oriented normal to the substrate surface.<sup>5</sup> However, the FWHMs of the x-ray  $\theta/2\theta$  scans determined from low and high temperature samples are 0.22° and 0.18°, respectively, suggesting an increase in the grain size at a high growth temperature. The  $\omega$  rocking curve indicates a better vertical alignment of crystal columns, a decrease from 1.2° to 0.85°, for a sample grown at a high temperature. As a result, higher growth temperature improves the quality of the grain core and reduces the grain boundary width.

The optical functions of the grain boundary region have been studied by using the spatially resolved EELS. Despite the fact that the films are found to be highly inhomogeneous, they exhibit a similar refractive index profile at the grain boundary. Figure 1 illustrates the typical line spectra of the refractive index scanned across the grain boundary of the film grown at 700 °C. An excitonic resonance feature is clearly observed at the energy of  $\sim 3.2$  eV in the interior region of the grain. However, as the electron probe beam is moving toward the grain boundary, the excitonic structure gradually diminishes. In addition, the slight decrease of the value of  $n$  at low photon energy suggests a reduction of the local density of the film at the grain boundary. The extinction coefficient (not shown) at the grain boundary increases below the band gap indicating that a substantial amount of interfacial defect states have been generated. Photon scattering is caused by the multiple light reflections that are due to the refractive index difference between the grain and grain boundary.<sup>5</sup> The light scattering power of the grain boundary can, therefore, be understood by examining the scattering factor, which is defined as the ratio of the integrated area of the refractive index spectrum measured at a specific point to that of the spectrum acquired from the grain interior. The integration is carried out from 3 to 3.3 eV, which essentially covers the entire emission spectrum of the ZnO random laser. If the ratio is greater than 1, the grain boundary reflects

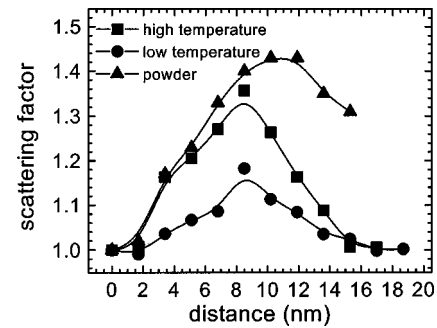


FIG. 2. The scattering factor of the high (square) and low (circle) temperature films. The inverted triangle indicates the factor obtained from the ZnO powder (triangle).

photons. On the other hand, light transmits when the ratio is smaller than 1. The results averaged from ten different site measurements are plotted in Fig. 2. It is seen that a bell-shaped profile, with a width of  $\sim 10$  nm, has been developed in the proximity of the grain boundary, which effectively scatters photons. The evolution of the layer remains uncertain. However, it is speculated that the space charge region given rise at the grain boundary is the likely cause.<sup>10</sup> It has been widely reported that a potential barrier is present at the grain boundary region due to the imbalance of the positive and negative charges. This barrier distorts the local band structure and therefore affects the electron transitions.<sup>7</sup> Considering that the carrier concentration and electron mobility of the film are  $8 \times 10^{18}/\text{cm}^3$  and  $3.1 \text{ cm}^2/\text{Vs}$ , the depletion width is determined to be 9.5 nm by assuming the trap density is  $7 \times 10^{12}/\text{cm}^2$  (Ref. 10), which is comparable to that of the measured reflective layer.

A similar bell-shaped profile of the scattering factor for the low temperature sample is also given in Fig. 2. The height and the width of the layer are found to be lower and wider than that of the high temperature. One might expect the high temperature sample to have a higher scattering power by comparing the two profiles. It is assumed the reduction of the light scattering factor for the low temperature sample is due to the inferior structural quality of the grain core, which lowers the refractive index. A lower substrate temperature impedes the surface diffusion of the clusters and, therefore, promotes the evolution of defects within the grains during the course of deposition.

The scattering activity of the ZnO films has also been measured by the CBS method.<sup>3,4</sup> We have estimated that the scattering mean free paths of the high and low temperature samples are  $2.4 \lambda$  and  $4.1 \lambda$ , respectively. The finite thickness of the films has been taken into account. The CBS results, in fact, indicate that the high temperature sample has a stronger scattering than that of the low temperature sample, which agrees well with the scattering factor profile. We also have examined the mapping of the refractive index dispersion of the ZnO powder that is reported to have laser action (Fig. 2). It is found the excitonic structure of the grain interior is similar to that of the low temperature sample. However, the low packing density of the powder has made a notable air gap,  $\sim 3$  nm wide, exists between two adjacent grains, which greatly facilitates the refractive index mismatch between the

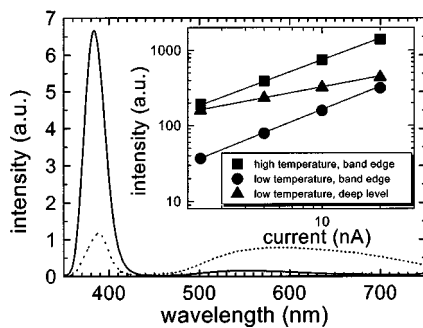


FIG. 3. The CL spectra of the high (solid) and low (short dash) temperature samples. The inset shows the excitation power dependence of CL emissions. The band edge emissions of both the high (square) and low (circle) temperature samples show a linear current dependence at constant accelerating voltage. However, the deep level emission of the low temperature (triangle) sample shows a sublinear relationship.

grain and grain boundary. The scattering mean free path is measured to be  $1.2 \lambda$ . Therefore, our results have clearly demonstrated that the grain boundary is responsible for the light scattering and the self-formation of laser cavities.

The CL has been used for studying the optical properties of the films. The high and low temperature samples, as shown in Fig. 3, both exhibit band edge emission as well as different intensities of deep-level emissions. In addition, the intensity of the band edge emission is improved with the deposition temperature. It is known that the band edge and deep level emissions of II–VI and III–V semiconductors follow different excitation power dependences.<sup>11</sup> The intensity of the excitonic emission increases linearly or superlinearly with the excitation power while that of the deep level emission goes after a sublinear dependence. The excitation power dependence measurement is carried out at a constant beam voltage of 6 kV with a different beam current and the results are plotted in the inset of Fig. 3. The band edge emission of two films clearly show a linear relationship with the beam current indicating that the emissions are in fact excitonic related. It also confirms the EELS results that a high temperature sample is considerably more excitonic. However, the deep level emission of the low temperature film gradually decreases with an increasing beam current. Optical pump lasing experiments have been carried out at room temperature using a triple harmonic Nd:YAG laser.<sup>12</sup> It is found that the lasing threshold of the high temperature film is  $450 \text{ kW/cm}^2$ , which is comparable to that of the reported value.<sup>3</sup> The low temperature film, on the other hand, does not lase.

We propose a qualitative model to elucidate the lasing in polycrystalline ZnO. The random laser action is largely fa-

cilitated by two factors: the intrinsic optical gain of the active medium and the laser cavity geometry. The former determines the lasing threshold and is strongly influenced by the quality of the grain interior. Higher crystal quality leads to higher optical gain as well as lower lasing threshold. However, the latter factor, which depends on the optical scattering, is largely controlled by the grain size and the scattering factor at the grain boundary. In optical pumping, stimulated emission occurs in the ZnO when the excitation is above the threshold. Instead of inducing optical loss, the strong optical scattering actually localizes photons and thereby promotes the formation of laser cavities with a ring-like geometry. If the active medium has a very high optical gain, laser action occurs once the light amplification exceeds the loss in the cavities. Therefore, it is expected that the grain and grain boundary are necessary to work together in order to shape the light emission in the random laser.

In short, the optical properties of polycrystalline ZnO thin films have been studied by spatially resolved EELS, CBS, and CL. A reflective layer of 9–12 nm has been observed in the proximity of the grain boundaries, which affects the optical scattering in the active medium. It is found that the combination of the grain and grain boundary is essential to navigate the laser action in the random ZnO.

The authors would like to thank Dr. Z. Q. Zhang and Dr. Y. Y. Wang for useful discussions. This research was supported by the City University of Hong Kong through the RGC Competitive Earmarked Research Grant No. 9040434, the NSFC/RGC Joint Research Scheme (9050138), and the Direct Allocation Grant No. 7100034.

<sup>1</sup>Z. K. Tang, G. K. L. Wong, P. Yu, M. Kawasaki, A. Ohtomo, H. Koinuma, and Y. Segawa, *Appl. Phys. Lett.* **72**, 3270 (1998).

<sup>2</sup>D. M. Bagnall, Y. F. Chen, Z. Zhu, T. Yao, S. Koyama, M. Y. Shen, and T. Goto, *Appl. Phys. Lett.* **70**, 2230 (1998).

<sup>3</sup>H. Cao, Y. G. Zhao, H. C. Ong, S. T. Ho, J. Y. Dai, J. Y. Wu, and R. P. H. Chang, *Appl. Phys. Lett.* **73**, 3656 (1998).

<sup>4</sup>H. Cao, Y. G. Zhao, S. T. Ho, E. W. Seelig, Q. H. Wang, and R. P. H. Chang, *Phys. Rev. Lett.* **82**, 2278 (1999).

<sup>5</sup>H. C. Ong, J. Y. Dai, K. C. Hung, G. T. Du, and S. T. Ho, *Appl. Phys. Lett.* (accepted for publication).

<sup>6</sup>A. Madan, I. W. Kim, S. C. Cheng, P. Yashar, V. P. Dravid, and S. A. Barnett, *Phys. Rev. Lett.* **78**, 1743 (1997).

<sup>7</sup>R. F. Egerton, *Electron Energy Loss Spectroscopy in the Electron Microscope* (Plenum, New York, 1986).

<sup>8</sup>H. Mulleijans and R. H. French, *J. Phys. D* **29**, 1751 (1996).

<sup>9</sup>X. B. Zhang, H. K. Won, and S. K. Hark, *Appl. Phys. Lett.* **73**, 3238 (1998).

<sup>10</sup>V. Srikant, V. Sergo, and D. R. Clarke, *J. Am. Ceram. Soc.* **78**, 1931 (1995); *J. Am. Ceram. Soc.* **78**, 1935 (1995).

<sup>11</sup>T. Schmidt, K. Lischka, and W. Zulehner, *Phys. Rev. B* **45**, 8989 (1992).

<sup>12</sup>H. C. Ong, M. K. Chan, and K. Y. Cheung (unpublished results).